

# PEGylated Graphene Oxide-Mediated Protein Delivery for Cell Function Regulation

He Shen,<sup>†,§,⊥,¶</sup> Min Liu,<sup>†,¶</sup> Huixin He,<sup>‡</sup> Liming Zhang,<sup>†</sup> Jie Huang,<sup>†</sup> Yu Chong,<sup>†</sup> Jianwu Dai,<sup>†</sup> and Zhijun Zhang<sup>\*,†</sup>

<sup>†</sup>Division of Nanobiomedicine, Suzhou Institute of Nano-tech and Nano-bionics, Chinese Academy of Sciences, 398 Ruoshui Road, Suzhou, 215123, China

<sup>‡</sup>Chemistry Department, Rutgers University, 73 Warren St., Newark, New Jersey 07102, United States

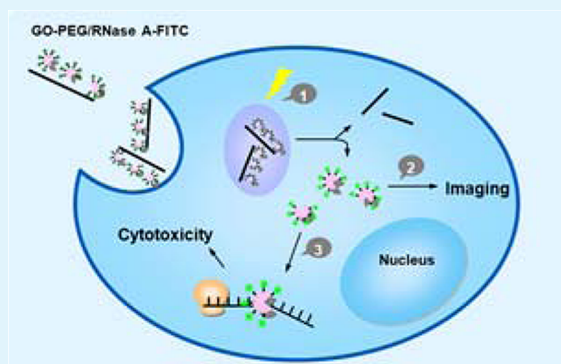
<sup>§</sup>University of Chinese Academy of Sciences, 19(A) Yuquan Road, Beijing, 100039, China

<sup>⊥</sup>Institute of Chemistry, Chinese Academy of Sciences, Zhong Guan Cun Bei Yi Jie 2, Beijing, 100190, China

## Supporting Information

**ABSTRACT:** Delivery of proteins into cells may alter cellular functions as various proteins are involved in cellular signaling by activating or deactivating the corresponding pathways and, therefore, can be used in cancer therapy. In this study, we have demonstrated for the first time that PEGylated graphene oxide (GO) can be exploited as a nanovector for efficient delivery of proteins into cells. In this approach, GO was functionalized with amine-terminated 6-armed polyethylene glycol (PEG) molecules, thereby providing GO with proper physiological stability and biocompatibility. Proteins were then loaded onto PEG-grafted GO (GO-PEG) with high payload via noncovalent interactions. GO-PEG could deliver proteins to cytoplasm efficiently, protecting them from enzymatic hydrolysis. The protein delivered by GO-PEG reserves its biological activity that regulates the cell fate. As a result, delivery of ribonuclease A (RNase A) led to cell death and transport of protein kinase A (PKA) induced cell growth. Taken together, this work demonstrated the feasibility of PEGylated GO as a promising protein delivery vector with high biocompatibility, high payload capacity and, more importantly, capabilities of protecting proteins from enzymatic hydrolysis and retaining their biological functions.

**KEYWORDS:** graphene oxide, loading capacity, protein delivery, cellular uptake, enzymatic hydrolysis, regulation of cell function



## INTRODUCTION

Proteins play an important role in regulation of gene expression and cellular signaling pathways<sup>1</sup> and, therefore, represent tremendous opportunities in terms of biotherapeutics,<sup>2–4</sup> vaccines,<sup>5</sup> tissue engineering,<sup>6</sup> and embryonic stem (ES) cell regulation.<sup>7</sup> Protein-based biotherapy especially metabolic manipulation applications have several advantages over conventional chemotherapy, such as serving a highly specific set of cell functions and having less adverse effects and the capability of escaping immune responses.<sup>8,9</sup> However, poor cellular uptake efficiency, limited transporting into tissues (in particular across blood–brain barrier), and enzymatic hydrolysis have severely restricted biomedical applications of functional proteins. To overcome these hampers, various strategies, such as conjugating proteins with a transduction domain<sup>10</sup> and other bacterial proteins,<sup>11</sup> have been developed. Although using recombinant fusion protein is a typical strategy for transporting proteins, its synthesis is rather complicated.

Recently, various nanomaterials, such as liposomes,<sup>12,13</sup> polymers,<sup>14</sup> carbon nanotubes,<sup>15</sup> and silica nanoparticles,<sup>16,17</sup> have been employed as carriers for delivery of therapeutic

proteins with different degrees of success. For example, Dai et al.<sup>15</sup> explored carbon nanotubes as intracellular protein transporters. In their work, proteins were nonspecifically adsorbed on the sidewalls of acid-oxidized single walled carbon nanotubes (SWNTs) and then transported into living cells. They revealed that the cellular-uptake mechanism is an energy dependent, clathrin mediated endocytosis. In addition, Huang and colleagues<sup>13</sup> used lipid-apolipoprotein nanoparticles to specifically deliver therapeutic proteins into tumor tissue; the protein drug loaded nanoparticles exhibited improved biocompatibility and reduced aggregation in vivo. Meanwhile, the lipid nanoparticles can be modified with various ligands to enhance the targeting ability and maintain biological stability in vivo. However, how to improve the loading capacity of protein drugs and the chemical and biological stability of protein delivered in the biological environment still remains a great challenge for researchers.

**Received:** September 9, 2012

**Accepted:** October 30, 2012

**Published:** October 30, 2012



In recent years, functional graphene oxide (GO) has been extensively investigated for biomedical applications,<sup>18,19</sup> such as nanocarriers for delivery of chemical drugs and genes into cells due to its excellent biocompatibility, low toxicity, and high payload capacity.<sup>20–23</sup> However, to the best of our knowledge, exploration of GO for delivery of functional proteins has not been reported. In this work, we have developed GO modified with polyethylene glycol (GO-PEG) as a nanovector for efficient delivery of proteins into cells. We have demonstrated that the GO protects the protein against enzymatic hydrolysis and that the proteins delivered into cells still retain their functions for regulating cell apoptosis or proliferation.

## ■ EXPERIMENTAL SECTION

**Materials.** Native graphite flake was purchased from Alfa Aesar; fluorescein isothiocyanate (FITC), chloroquine, ribonuclease A (RNase A), and protein kinase A (PKA) were obtained from Sigma-Aldrich. RPMI 1640 cell culture medium, fetal bovine serum (FBS), and 0.25% Trypsin-ethylenediaminetetraacetic acid (EDTA) were acquired from Gibco BRL (Grand Island, NY). Other reagents were obtained from China National Medicine Corporation and used as received. Milli-Q water was used in all experiments.

**Instrumentation.** UV–vis spectra and fluorescence spectra were collected with Shimadzu UV-2550 spectrophotometer and Hitachi F-4600 fluorescence spectrometer, respectively. Morphological analyses were carried out on a Veeco Dimension 3100 atomic force microscope. Confocal imaging was taken on a Nikon A1. Water-Soluble Tetrazolium Salts Cell Proliferation and Cytotoxicity Assay Kit (WST) was performed using a microplate reader (Perkin-Elmer Victor X4). Flow cytometry analysis (FACS) was performed by FACSaria II (Becton Dickinson).

**Synthesis of PEGylated GO.** GO was prepared by modified Hummers method<sup>21,24</sup> and then converted to carboxylated GO according to our previous work.<sup>21</sup> After that, GO was modified by coupling the amino groups of amine-terminated six-armed polyethylene glycol (PEG) to the carboxyl groups of GO in the presence of *N*-ethyl-*N'*-(3-dimethylamino-propyl) carbodiimide hydrochloride (EDC) according to the protocol described previously by Liu et al.<sup>20</sup>

**Fluorescent Dye Labeling of Proteins.** Protein was labeled by fluorescein isothiocyanate (FITC) for intracellular fluorescence imaging of proteins. In brief, protein aqueous solution (10 mg/mL) was mixed with excess FITC predispersed in DMSO (dimethyl sulfoxide) and then reacted for 2 h at room temperature in dark. The resulting FITC-labeled protein was purified by dialysis. The concentration of the FITC labeled protein after dialysis was determined by BCA (bicinchoninic acid) protein assay kit.

**Protein Loading and Release.** FITC-labeled BSA was used as a model protein to investigate loading and release behavior of proteins. Protein loading onto GO-PEG was achieved by simply mixing BSA-FITC with aqueous solution of GO-PEG (0.25 mg/mL) at room temperature overnight in darkness. The unbound BSA-FITC was removed by filtration. The loading ratio ( $R_{\text{loading}}$ ) was calculated by checking fluorescence quenching according to the following equation:

$$R_{\text{loading}} = 1 - F_{\text{GO-PEG/BSA-FITC}}/F_{\text{BSA-FITC}} \quad (1)$$

To study the release behavior of proteins from GO, GO-PEG/BSA-FITC was added into different physiological solutions at 18 or 37 °C and kept stirring for different time periods. Fluorescence of FITC was recovered upon release of the FITC-labeled protein from GO sheet. Therefore, protein release ratio ( $R_{\text{releasing}}$ ) can be quantified by the following equation:

$$R_{\text{releasing}} = (F_{\text{releasing}} - F_{\text{GO-PEG/BSA-FITC}}) / (F_{\text{BSA-FITC}} - F_{\text{GO-PEG/BSA-FITC}}) \quad (2)$$

where  $F_{\text{BSA-FITC}}$  and  $F_{\text{GO-PEG/BSA-FITC}}$  represent the fluorescence of BSA-FITC and GO-PEG/BSA-FITC, respectively.  $F_{\text{releasing}}$  stands for

the fluorescence of GO-PEG/BSA-FITC in different physiological solutions.

Similarly, the other two protein models, RNase A and PKA, were loaded onto GO sheets. In brief, FITC-labeled RNase A or PKA was mixed with GO-PEG aqueous solution (0.25 mg/mL) at room temperature and kept overnight in darkness, followed by removal of excess free proteins by filtration.

**Protein Stability against Enzymatic Digestion.** The role of GO-PEG in protecting proteins from enzymatic cleavage was probed by trypsin digestion analysis. Briefly, trypsin aqueous solution (0.125%) was introduced into each BSA-FITC or GO-PEG/BSA-FITC samples with the same BSA concentration, 0.08 mg/mL, and the enzyme reaction was performed at 37 °C for 1, 3, and 6 h, respectively. All samples were heated to 100 °C for 10 min to stop the reaction. Immediately after trypsin digestion, the trypsin-digested GO-PEG/BSA-FITC and BSA-FITC were analyzed by sodium dodecyl sulfate-polyacrylamide gel electrophoresis (SDS-PAGE), to determine the amount of intact proteins.

**Cell Proliferation and Cytotoxicity Assay.** WST assay was performed to investigate the cell proliferation and cytotoxicity. HeLa and MCF-7 cells were cultured in RPMI 1640 medium with 10% serum under a fully humidified atmosphere at 37 °C with 5% CO<sub>2</sub>. For WST cell proliferation and cytotoxicity assays, the cells were seeded in 96-well plates at the density of  $7 \times 10^3$  cells per well and incubated for 48 h. Cell viability was then measured by means of WST assay according to the manufacturer suggested procedure.

**Flow Cytometric Analysis of Apoptosis.** Flow cytometric analysis (FACS) was performed on FACSaria II flow cytometer at an excitation wavelength of 488 nm and an emission wavelength of 610 nm, for 10 000 cells per sample. Apoptotic cell was analyzed by staining with propidium iodide (PI). PI is an agent which could label the apoptotic or necrotic cells, specifically. Briefly, the samples were washed with PBS for three times and suspended in 1 mL of buffer. FACS was performed immediately after adding PI.

**Cellular Uptake.** HeLa and MCF-7 cells cultured in 24-well plates were incubated with a GO-PEG/BSA-FITC suspension for 1, 5, and 18 h and then rinsed with PBS. The concentration of BSA-FITC loaded on GO-PEG was 30 μg/mL. Finally, confocal fluorescence microscopy images were captured to investigate cellular uptake of GO-PEG/BSA-FITC. Free BSA-FITC with the same concentration was also incubated with cells as a control.

## ■ RESULTS AND DISCUSSION

In our strategy, GO was chemically conjugated with amine-terminated 6-arm PEG and then loaded with three different types of proteins, bovine serum albumin (BSA), ribonuclease A (RNase A), and cyclic-AMP dependent protein kinase A (PKA) via physisorption, respectively. The schematic illustration (Figure 1) shows the formation of GO-PEG/protein complex. In all cases, the proteins were covalently bound to fluorescein isothiocyanate (FITC) and then loaded onto GO sheet. The roles of FITC in this work are two fold: acting as a fluorescent labeling agent for cellular imaging and facilitating adsorption of the proteins onto GO via  $\pi$ - $\pi$  stacking and other molecular interactions. FITC-labeled BSA was first used as a model protein to investigate loading and release behavior of proteins and the intracellular uptake. Taking RNase A and PKA as active cargo proteins, we further investigated the cellular uptake of functional protein-GO complexes and the regulation of cell functions by influencing intracellular protein synthesis and signaling pathways.<sup>9</sup> The results presented in the current work may open up new possibilities for developing GO-based protein delivery systems for protein therapeutics as well as regulating cell functions.

**Synthesis and Characterization of GO-PEG/BSA-FITC.** PEG was conjugated to GO via formation of amide bonds in the presence of EDC as previously reported,<sup>18</sup> followed by

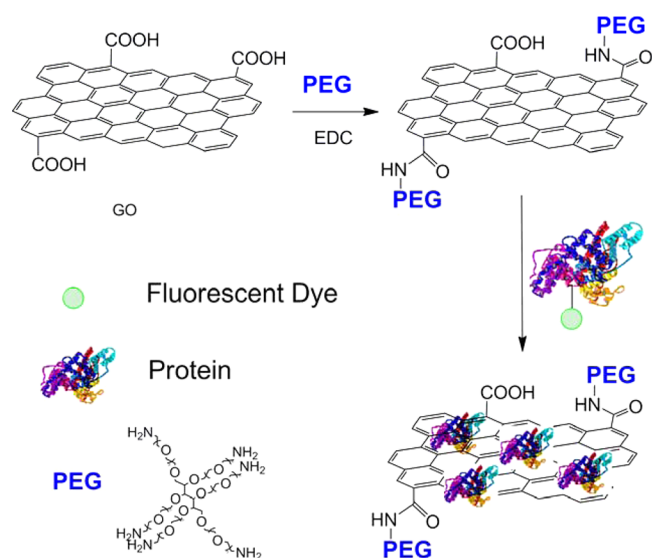


**Figure 1.** Schematic diagram showing formation of GO-PEG/BSA-FITC complex.

loading of FITC labeled protein via physical adsorption. GO and GO-PEG was further confirmed by infrared (IR) and Raman spectroscopy (see Figure S1 in the Supporting Information). In IR spectra, a pronounced C–H band of the PEG was observed, indicating successful conjugation of PEG onto the GO sheet. As reported in previous literature,<sup>20</sup> grafting PEG molecules to GO can render its physiological stability and biocompatibility. Meanwhile, fluorescent molecule, FITC, serves as labeling dye of proteins. We also measured the change of the  $\zeta$ -potential of protein, FITC labeled protein, GO, GO-PEG, and GO-protein complex (see Table S1 in the Supporting Information). The data indicated the successful formation of GO-protein complex and good stability of GO-protein complex in aqueous solution. The morphology of GO-PEG before (Figure 2) and after loading of BSA-FITC was investigated by atomic force microscopy (AFM). GO-PEG is less than 200 nm in lateral width and  $\sim 1.8$  nm in thickness (see Figure S2 in the Supporting Information), which is a little thicker than GO sheets (about 1 nm). Mixing of the GO-PEG with BSA-FITC in solution overnight leads to further increase

in the thickness to about 3.6 nm, suggesting successful loading of the BSA-FITC onto the GO sheets, forming GO-PEG/BSA-FITC complexes. Thus-formed GO-protein complexes were further characterized by UV–vis and fluorescence spectroscopies. In the UV–vis spectra, two absorption peaks appear at  $\sim 495$  and  $\sim 230$  nm, characteristic of FITC and GO, respectively (Figure 3A), indicating successful loading of the dye-tagged protein on the GO sheet. Upon adsorption of BSA-FITC to GO-PEG, the fluorescence of FITC was completely quenched due to efficient fluorescence resonance energy transfer (FRET) between GO and FITC,<sup>25</sup> indicating the strong interaction between BSA-FITC and GO-PEG (Figure 3B). The protein molecules, we think, are adsorbed onto the GO surface via  $\pi$ – $\pi$  stacking and hydrophobic and electrostatic interactions between GO and the FITC-tagged protein.<sup>26</sup>

**Loading and Release Behavior of Protein.** Loading and release behavior of protein is very important for practical applications of a drug delivery system; therefore, we monitored the loading and release process of the protein to and from GO by fluorescence spectroscopy. The loading capacity ( $R_{\text{loading}}$ ) increases with BSA-FITC concentration following a linear relationship (Figure 4A), quantified by the following equation:

$$R_{\text{loading}} (\%) = 0.2694 \times C_{\text{BSA-FITC}} (\mu\text{g/mL}) - 3.8463 \quad (3)$$

Owing to the large surface area of GO, the loading capacity of BSA-FITC is extremely high, being 350% (w/w) in our experimental condition, which is much higher than that of other commonly reported nanovectors such as liposomes (loading efficiency 60–90%).<sup>13,27</sup> It was found that loading rate of BSA on GO sheets was dependent to the concentrations of BSA-FITC, indicating that the loading is a diffusion-driven process.<sup>17</sup> The loading process of the FITC-labeled proteins onto GO is very fast, as evidenced by the observation of complete fluorescence quenching immediately after mixing GO-PEG with BSA-FITC in aqueous solution. As shown in Figure 4B, nearly half of the protein cargo was loaded onto GO in 1 min after mixing BSA-FITC with GO-PEG. The loading process continued and almost completed within 4 h. Nearly 80% BSA-FITC was loaded on the GO surface upon adsorption equilibrium. The high payload of proteins onto the GO sheets

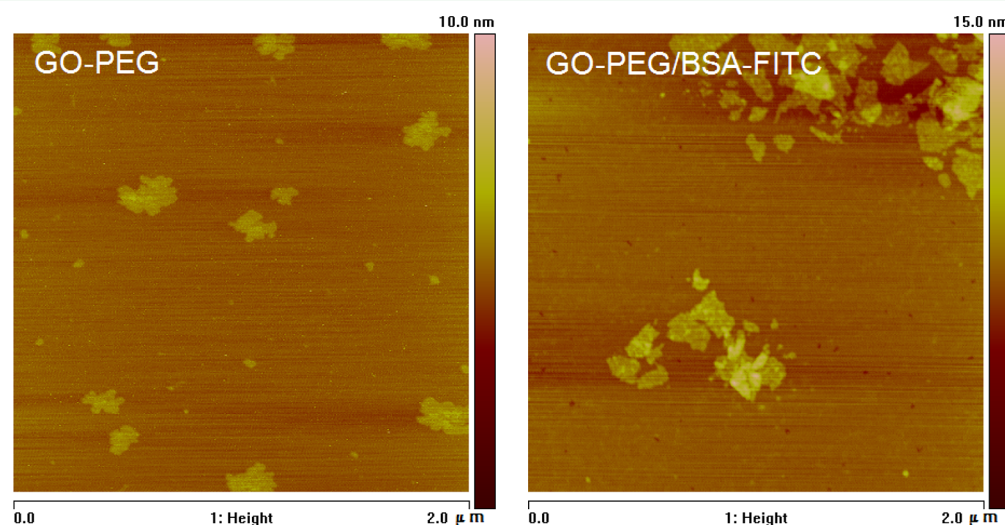


**Figure 2.** AFM images of GO-PEG (A) before and (B) after being loaded with BSA-FITC.

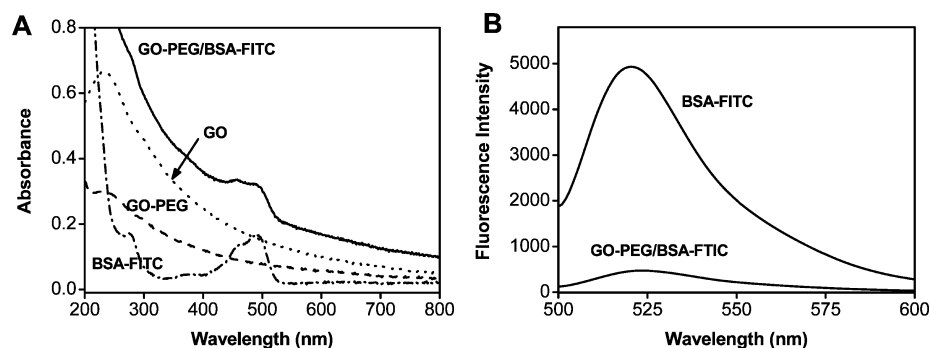


Figure 3. (A) UV-vis and (B) fluorescence spectra of GO-PEG before and after being loaded with BSA-FITC.

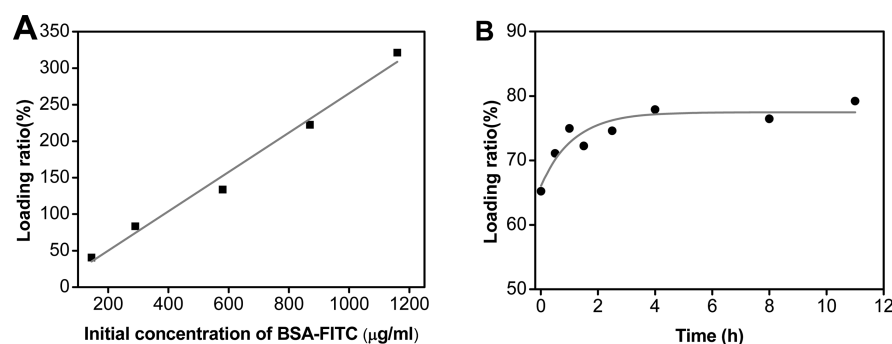


Figure 4. (A) Plot of loading ratio of BSA-FITC on GO-PEG versus initial concentration of BSA-FITC. (B) Plot of loading ratio of BSA-FITC on GO-PEG versus adsorption time.

is due to its strong  $\pi$ - $\pi$  interaction with large surface area of GO.

Next, the release of adsorbed protein from GO surface at 18 and 37 °C was studied in phosphate buffer solution (PBS) and cell culture medium (RPMI 1640 with and without 10% serum), respectively. As shown in Figure 5, slow but steady

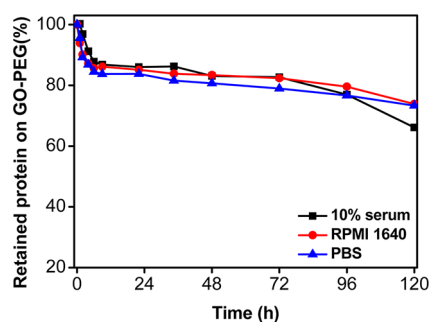
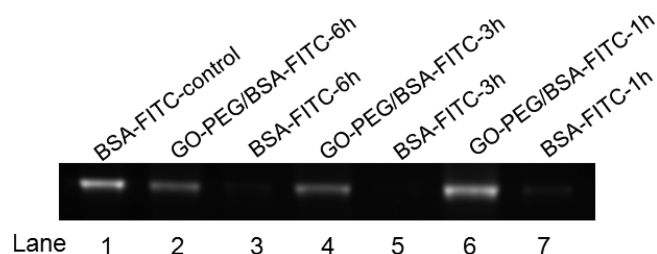


Figure 5. Release behavior of BSA-FITC from GO-PEG at 18 °C in PBS and cell culture medium with and without 10% serum, respectively.

release of BSA from GO was observed. In the first 6 h, 13% of the protein was released from GO-PEG in PBS buffer at 18 °C. After 5 days, total released protein reached nearly 20%. The release profiles of the protein from GO-PEG surface in the different physiological conditions are similar. It is worth noting that hardly any protein was released from GO surface in pure water over 120 h (see Figure S4D in the Supporting Information), indicating the strong noncovalent interaction between FITC labeled proteins and GO sheets.<sup>20</sup> The release behavior of BSA from GO at 37 °C over a period of 48 h was also studied in different media. Nearly 25% of the adsorbed

BSA-FITC was released gradually from GO in PBS during the first 20 h (see Figure S4A in the Supporting Information). The maximum release ratio is nearly 50% in 48 h. The release behavior of BSA-FITC from GO-PEG in cell culture medium (see Figure S4B, S4C in the Supporting Information) is similar to that in PBS buffer. The release ratio of BSA-FITC in RPMI 1640 containing 10% serum and RPMI 1640 was 41.7% and 35.9%, respectively. As the release of adsorbed proteins from the GO surface needs energy, high temperature condition will facilitate the release of BSA from the GO surface; therefore, temperature dependent release profiles of BSA-FITC from GO-PEG were observed. The favorable interactions between the protein and the GO surface may be altered by other ionic species in the solution similar to what has been observed previously.<sup>17,26</sup>

**GO's Role in Protection of Proteins from Enzymatic Digestion.** As the efficacy of protein-based therapy also depends, to a large extent, on the stability of proteins against enzyme degradation,<sup>28</sup> we investigated the stability of proteins adsorbed on GO in the presence of protease in vitro. GO-protein complexes (GO-PEG/BSA-FITC) and free protein (BSA-FITC) were treated with a protein-digesting enzyme, trypsin, at 37 °C, respectively. SDS-PAGE analysis reveals that, after treatment for the first 1 h, no discernible change of the amount of intact protein in the GO-PEG/BSA-FITC samples (Figure 6 Lane 6) was observed compared to the control sample (Figure 6 Lane 1). In contrast, the free BSA-FITC was completely digested after incubation with the enzyme for 1 h, as evidenced by the complete disappearance of the band with relative molecular weights of BSA in the trypsin-treated BSA-FITC samples. These results suggest that the BSA-FITC loaded on GO-PEG could be protected from enzymatic degradation. The mechanism for protection of protein from enzymatic cleavage by GO is not clear at this moment. It is very likely that



**Figure 6.** SDS-PAGE analysis of BSA-FITC without trypsin digestion (lane 1) and GO-PEG/BSA-FITC and free BSA-FITC with trypsin cleavage for 1 h (lane 6 and 7), 3 h (lane 4 and 5), and 6 h (lane 2 and 3), respectively.

the constraint of protein on GO-PEG would prevent the protein from cleavage due to steric hindrance of the GO sheet that prevents trypsin from binding to the protein to initiate enzymatic digestion, similar to what was observed in the case of delivery of DNA by GO.<sup>29–31</sup> The current result clearly demonstrated that GO-PEG is able to protect proteins adsorbed from enzymolysis, which ensures that the biological functions of the delivered proteins can be largely preserved. It is also noted that, with increasing the enzyme digestion time, the amount of intact BSA protein also decreased gradually (Lane 2 and 4 in Figure 6), because the protein was desorbed gradually from GO surface and then hydrolyzed by trypsin, which is consistent with the BSA release characteristic described above.

**Cellular Uptake of the GO/Protein Complex.** As efficient cellular internalization is the key to drug delivery and therapy, we have studied the uptake of GO-PEG loaded with BSA-FITC by two cell lines (HeLa and MCF-7) by means of confocal fluorescence microscopy. FITC labeling facilitates a quick and reliable monitoring and tracking of the intracellular localization of the protein. The HeLa cells were stained with a nucleus staining dye, DAPI, which appears as blue color in dark

field. Cells treated with GO-PEG/BSA-FITC showed green fluorescence localized in cytoplasm after incubation for 18 h, while no fluorescence was observed for free BSA-FITC treated in the same way (Figure 7 and Figure S5A in the Supporting Information). Cellular uptake of BSA-FITC loaded on GO-PEG was significantly higher than that of free BSA-FITC, suggesting the important role of GO-PEG in transporting protein into the cells. Formation of GO-PEG/BSA-FITC complexes may facilitate escaping of BSA-FITC from endosomes and then release into the cytoplasm, as evidenced by observation of fluorescence of FITC mainly throughout the cytoplasm. The efficient delivery of proteins into cytoplasm may be attributed to high payload of proteins on GO-PEG, which protects protein from enzymatic digestion. The mechanism of cell internalization of GO loaded with proteins is still unclear so far. Most recently, we demonstrated that GO may be taken up by cells via energy dependent, clathrin-mediated endocytosis.<sup>32</sup> Apparently, much work is desired to understand the cell entry mechanism and pathway of the proteins loaded on GO.

**Regulation of Cell Functions by GO Delivered Proteins.** Finally, we explored whether functional proteins released from GO-PEG still retains their biological activity *in vitro*. First, RNA-cleaving protein enzyme, ribonuclease A (RNase A, MW 13.7 kD), was chosen to study protein-modulated cell apoptosis. It is reported that RNase A can degrade mRNA and tRNA nonspecifically and, therefore, inhibit protein synthesis in cytoplasm,<sup>33</sup> which has a wide range of biological applications, such as antitumor, angiogenic, and allergy-inducing activities.<sup>9,34</sup> In order to understand regulation of cell functions by the proteins delivered by GO-PEG, we first checked the cytotoxicity of GO-PEG. WST result (Figure 8A) reveals that GO-PEG showed very low cytotoxicity after incubation with HeLa cells for 48 h. Meanwhile, incubation with the same concentration of free RNase A-FITC (150  $\mu\text{g}/$

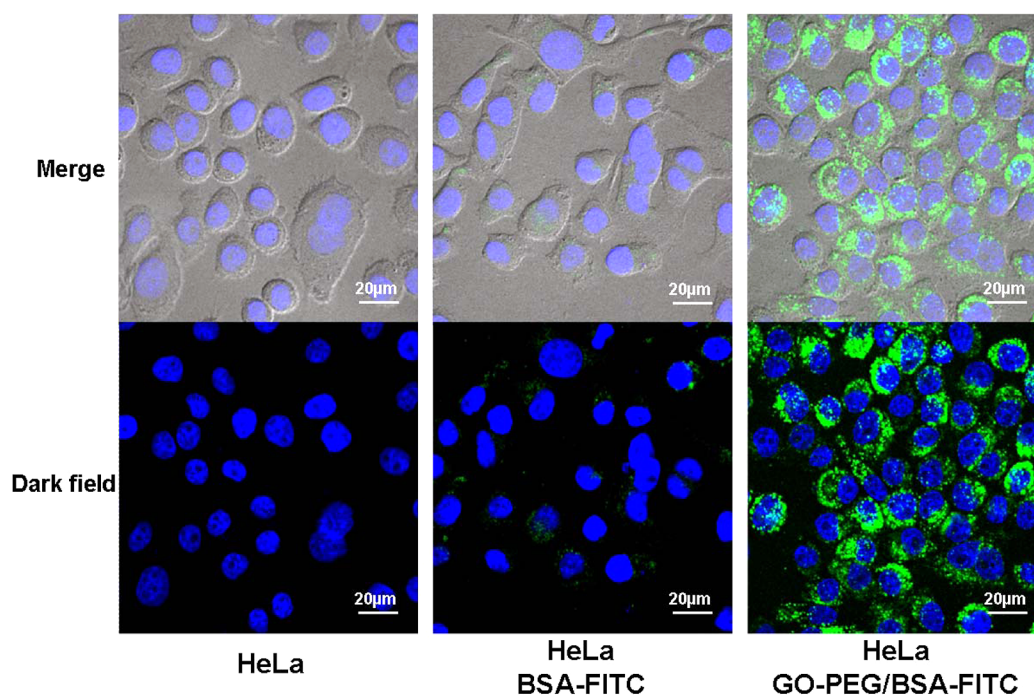


**Figure 7.** Confocal fluorescence microscopy images of HeLa cells before and after being incubated with free BSA-FITC and GO-PEG/BSA-FITC, respectively.

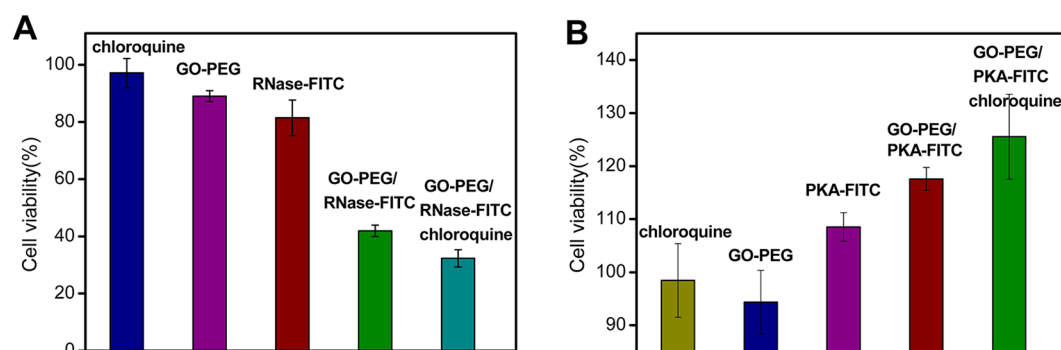


**Figure 8.** (A) Relative viability of HeLa cells after being incubated with chloroquine, GO-PEG, RNase A-FITC, GO-PEG/RNase A-FITC, and GO-PEG/RNase A-FITC with chloroquine pretreating, respectively. (B) Relative viability of MCF-7 cells after being incubated with chloroquine, GO-PEG, PKA-FITC, GO-PEG/PKA-FITC, and GO-PEG/PKA-FITC with chloroquine pretreating, respectively.

mL) leads to slight decrease in cell viability. In contrast, significant decreasing in cell viability was observed (about 42%), when HeLa cells were treated with GO-PEG/RNase A-FITC of the same protein concentration, which was well above the basal cytotoxicity caused by either GO-PEG or RNase A-FITC alone. To further enhance the protein release efficiency from endosome, chloroquine was used to trigger endosomal release of the internalized protein into cytoplasm. Chloroquine is an endosome disruption agent ascribable to increasing pH and osmotic pressure inside endosomes, which lead to endosome swelling and rupture eventually,<sup>35</sup> and result in enhancement of release. In our experiment, substantially enhanced apoptosis was observed when the HeLa cells were pretreated with 100  $\mu$ M chloroquine. Nearly 25% increase in cytotoxicity of GO-PEG delivered RNase A-FITC was shown in the presence of chloroquine. Moreover, to further support the result from the WST assay above, flow cytometry was performed with PI staining. Apoptosis was quantified by the rate of apoptotic HeLa cells. The FACS results (Figure S6 in the Supporting Information) indicated that no significant apoptosis was induced when cells were incubated with GO-PEG and chloroquine. Only 1.7% of HeLa cells treated with free RNase A-FITC exhibited apoptosis. In comparison, the induced cellular apoptosis was increased to 47.9% and 76.0% of cells incubated with GO-PEG/RNase A-FITC and GO-PEG/RNase A-FITC with chloroquine pretreated, respectively, which is consistent with the WST assay above. The WST and FACS data together indicated that GO-PEG/RNase A-FITC complexes were endocytosed into cells and then released from endosomes, finally diffused throughout the entire cytoplasm. More importantly, the FITC marked RNase A delivered into cell by GO-PEG retains its biological activity resulting in significant cell apoptosis. Compared to other nanovectors, for example, carbon nanotubes,<sup>15</sup> generic intracellular transporters for various types of proteins ( $\leq 80$  kD), can efficiently transport proteins ( $\leq 80$  kD) inside various mammalian cells via endocytosis pathway. Dai and his co-workers reported that the cell apoptosis induced by Cyt-C alone was about 10%, which was lower than that of transporting by SWNTs (15%). In our work, GO-PEG could efficiently deliver various proteins to different cell lines leading to high levels of cell apoptosis (50%).

We further employed another protein model, protein kinase A (PKA), to elucidate the influence of functional proteins delivered by GO-PEG on the signaling pathways in cell. PKA plays a major role in PKA/B-Raf signaling pathways, leading to proliferation of cells in cytosol.<sup>36</sup> Delivery of PKA into

cytoplasm would increase the activity of PKA-regulated pathways, leading to cell growth. GO-PEG/PKA-FITC (20  $\mu$ g/mL) and free PKA-FITC (as a control) with the same protein concentration were introduced to MCF-7 cells, respectively. We observed significantly enhanced cell growth by incubating GO-PEG/PKA-FITC with MCF-7 cells for 48 h (Figure 8B). This could occur only when PKA-FITC is delivered into the cells and retains its bioactivity. Pretreatment of MCF-7 cells by chloroquine leads to more significant cell proliferation due to more efficient endosome release of the internalized GO-PEG/PKA-FITC. In contrast, no noticeable cell proliferation was observed when the cells were incubated with free PKA-FITC. Taken together, these results have demonstrated clearly that the GO-PEG-based protein delivery system ameliorates protein stability against enzymatic degradation and biological activity of regulating cell fate.

## CONCLUSIONS

In summary, we have demonstrated the feasibility of PEG-modified GO as a biocompatible and efficient nanovector for loading and delivery of proteins into cytoplasm and that GO-PEG prevents the proteins from enzymatic hydrolysis. We further show that the proteins delivered by GO-PEG retain their biological functions to induce apoptosis (by GO-PEG/RNase A-FITC) or cell proliferation (by GO-PEG/PKA-FITC). Collectively, this work provides insight into rational design of efficient GO-based protein delivery systems for protein therapy and metabolic manipulation.

## ASSOCIATED CONTENT

### Supporting Information

Infrared (IR) spectra, Raman spectra of GO, thickness distribution of GO-protein complex, AFM image of BSA-FITC, release behavior of the proteins absorbed on GO, cellular uptake of the GO-protein complexes, FACS analysis, and zeta potentials. This material is available free of charge via the Internet at <http://pubs.acs.org/>.

## AUTHOR INFORMATION

### Corresponding Author

\*Tel: 86-512-62872556. Fax: 86-512-62603079. E-mail: zjzhang2007@sinano.ac.cn.

### Author Contributions

<sup>¶</sup>These authors contributed equally to this work. The manuscript was written through contributions of all authors.

All authors have given approval to the final version of the manuscript.

## Notes

The authors declare no competing financial interest.

## ACKNOWLEDGMENTS

This work was supported by the National Natural Science Foundation of China (No. 21073224). The authors gratefully acknowledge the support of K. C. Wong Education Foundation, Hong Kong.

## REFERENCES

- (1) Sherr, C. J. *Science* **1996**, *274*, 1672–1677.
- (2) Gao, Z. Q.; Han, B. H.; Shen, J.; Gu, A. Q.; Qi, D. J.; Huang, J. S.; Shi, C. L.; Xiong, L. W.; Zhao, Y. Z.; Jiang, L. Y.; Wang, H. M.; Chen, Y. R. *Exp. Ther. Med.* **2011**, *2*, 811–815.
- (3) Wang, C. Y.; Mayo, M. W.; Baldwin, A. S., Jr. *Science* **1996**, *274*, 784–787.
- (4) Shen, F.; Kirmani, K. Z.; Xiao, Z. M.; Thirlby, B. H.; Hickey, R. J.; Malkas, L. H. *J. Cell. Biochem.* **2011**, *112*, 756–760.
- (5) Shi, L.; Sings, H. L.; Bryan, J. T.; Wang, B.; Wang, Y.; Mach, H.; Kosinski, M.; Washabaugh, M. W.; Sitrin, R.; Barr, E. *Clin. Pharm. Ther.* **2007**, *81*, 259–264.
- (6) Baldwin, S. P.; Saltzman, W. M. *Adv. Drug. Rev.* **1998**, *33*, 71–86.
- (7) Kim, D.; Kim, C. H.; Moon, J. I.; Chung, Y. G.; Chang, M. Y.; Han, B. S.; Ko, S.; Yang, E.; Cha, K. Y.; Lanza, R.; Kim, K. S. *Cell Stem Cell* **2009**, *4*, 472–476.
- (8) Leader, B.; Baca, Q. J.; Golan, D. E. *Nat. Rev.* **2008**, *7*, 21–39.
- (9) Andraday, C.; Sharma, S. K.; Chester, K. A. *Immunotherapy* **2011**, *3*, 193–211.
- (10) Schwarze, S. R.; Ho, A.; Vocero-Akbani, A.; Dowdy, S. F. *Science* **1999**, *285*, 1569–1572.
- (11) Galan, J. E.; Collmer, A. *Science* **1999**, *284*, 1322–1328.
- (12) Park, S. J.; Choi, S. G.; Davaa, E.; Park, S. J. *Int. J. Pharm.* **2011**, *415*, 267–272.
- (13) Kim, S. K.; Foote, M. B.; Huang, L. *Biomaterials* **2012**, *33*, 3959–3966.
- (14) Verheyen, E.; Wal, S. V. D.; Deschout, H. *J. Controlled Release* **2011**, *156*, 329–336.
- (15) Kam, N. W. S.; Dai, H. J. *J. Am. Chem. Soc.* **2005**, *127*, 6021–6026.
- (16) Bale, S. S.; Kwon, S. J.; Shah, D. A.; Banerjee, A.; Dordick, J. S.; Kane, R. S. *ACS Nano* **2010**, *4*, 1493–1500.
- (17) Slowing, I. I.; Trewyn, B. G.; Lin, V. S. Y. *J. Am. Chem. Soc.* **2007**, *129*, 8845–8849.
- (18) Wu, L.; Wang, J. S.; Feng, L. Y.; Ren, J. S.; Wei, W. L.; Qu, X. G. *Adv. Mater.* **2012**, *24*, 2447–2452.
- (19) Feng, L. Y.; Wu, L.; Wang, J. S.; Ren, J. S.; Miyoshi, D.; Sugimoto, N.; Qu, X. G. *Adv. Mater.* **2012**, *24*, 125–131.
- (20) Liu, Z.; Robinson, J. T.; Sun, X. M.; Dai, H. J. *J. Am. Chem. Soc.* **2008**, *130*, 10876–10877.
- (21) Zhang, L. M.; Xia, J. G.; Zhao, Q. H.; Liu, L. W.; Zhang, Z. J. *Small* **2010**, *6*, 537–544.
- (22) Chen, B.; Liu, M.; Zhang, L. M.; Huang, J.; Yao, J. L.; Zhang, Z. *J. Mater. Chem.* **2011**, *21*, 7736–7741.
- (23) Dong, H. F.; Gao, W. C.; Yan, F.; Ji, H. X.; Ju, H. X. *Anal. Chem.* **2010**, *82*, 5511–5517.
- (24) Hummers, W. S.; Offeman, R. E. *J. Am. Chem. Soc.* **1958**, *80*, 1339–1339.
- (25) Selvin, P. R. *Nat. Struct. Biol.* **2000**, *7*, 730–734.
- (26) Yang, X. Y.; Zhang, X. Y.; Liu, Z. F.; Ma, Y. F.; Huang, Y.; Chen, Y. S. *J. Phys. Chem. C* **2008**, *112*, 17554–17558.
- (27) Zaky, A.; Elbakry, A.; Ehmer, A.; Breunig, M.; Goepferich, A. *J. Controlled Release* **2010**, *147*, 202–210.
- (28) Torchilin, V. P.; Lukyanov, A. N. *Drug Discovery Today* **2003**, *8*, 259–266.
- (29) Tang, Z. W.; Wu, H.; Cort, J. R.; Buchko, G. W.; Zhang, Y. Y.; Shao, Y. Y.; Aksay, I. A.; Liu, J.; Lin, Y. H. *Small* **2010**, *6*, 1205–1209.
- (30) Wu, Y. R.; Phillips, J. A.; Liu, H. P.; Yang, R. H.; Tan, W. H. *ACS Nano* **2008**, *2*, 2023–2028.
- (31) Lei, H. Z.; Mi, L. J.; Zhou, X. J.; Chen, J. J.; Hu, J.; Guo, S. W.; Zhang, Y. *Nanoscale* **2011**, *3*, 3888–3892.
- (32) Huang, J.; Zong, C.; Shen, H.; Liu, M.; Chen, B.; Ren, B.; Zhang, Z. J. *Small* **2012**, *8*, 2577–2584.
- (33) Schein, C. H. *Nat. Biotechnol.* **1997**, *15*, 529–536.
- (34) Kim, W. C.; Lee, C. H. *Biochim. Biophys. Acta* **2009**, *1796*, 99–113.
- (35) Ogris, M.; Steinlein, P.; Kursa, M.; Mechtler, K.; Kircheis, R.; Wagner, E. *Gene Ther.* **1998**, *5*, 1425–1433.
- (36) Calipel, A.; Mouriaux, F.; Glotin, A. L.; Malecaze, F.; Faussat, A. M.; Mascarelli, F. *J. Biol. Chem.* **2006**, *281*, 9238–9250.